Competing activation mechanisms in epidemics on networks: Supplementary Information

Claudio Castellano[1,2] and Romualdo Pastor-Satorras[3]

[1]Istituto dei Sistemi Complessi (ISC-CNR), Via dei Taurini 19, I-00185 Roma, Italy
[2]Dipartimento di Fisica, "Sapienza" Università di Roma, P.le A. Moro 2, I-00185 Roma, Italy
[3]Departament de Física i Enginyeria Nuclear, Universitat Politècnica de Catalunya, Campus Nord B4, 08034 Barcelona, Spain

1 Details of SIS numerical simulations.

The numerical simulations of SIS dynamics have been performed in the standard rejection-free way [1]: At each time step one node from the list of infected vertices is chosen at random and removed; then, each of its neighbors is considered and, if healthy, infected with probability λ. Time is incremented by the inverse of the total number of occupied nodes. Substrate networks are created using the uncorrelated configuration model (UCM) [2].

Initially, all nodes are taken to be infected. No variation is expected for any finite fraction of infected nodes in the initial state. Spreading experiments, with a single infected vertex in the initial state, are an interesting topic for future work.

Results are averaged over many realizations (at least 10) of the dynamical process on a single network. We have not averaged over different network samples, because fluctuations in the various geometrical quantities (max k-core order, max k-core size, hub connectivity)

make averaged results less clear (see Ref. [3]).

The system sizes considered for larger γ are larger than for smaller values of γ. This is motivated by the need to increase the separation between $1/\sqrt{q_{max}}$ and $\langle q\rangle/\langle q^2\rangle$, in order to allow for a clear distinction between the two mechanisms.

2 Results for additional values of γ.

In Fig. S1 we report the results of additional simulations of the SIS model on uncorrelated power-law distributed networks with exponent γ, for values of γ different from those reported in the main text. These results confirm that the activation mechanism triggering the epidemic transition is the largest hub or the innermost maximum k-core, depending on whether γ is larger or smaller than $5/2$.

3 Degree distribution of the maximum k-core.

We study the topological properties of the maximum k-core in uncorrelated scale-free networks generated using the UCM model. We focus in particular on the average degree $\langle q_{k_S}\rangle$ of the maximum k-core, and on its maximum $q_{k_S}^{max}$ and minimum $q_{k_S}^{min} = k_S$ degree. In Fig. S2 we plot this quantities averaged over networks with different size N as a function of the network's maximum degree $q_{max} \sim N^{1/2}$. The networks considered have a degree exponent $\gamma = 2.5$. From this figure, we conclude that all the computed properties of the maximum k-core scale in the same way with the network size (i.e. are proportional to each other), indicating that the degree distribution remains rather narrow for any network size. This observation justifies the assumption that heterogeneous mean-field theory determines correctly the scaling of the epidemic threshold on the maximum k-core.

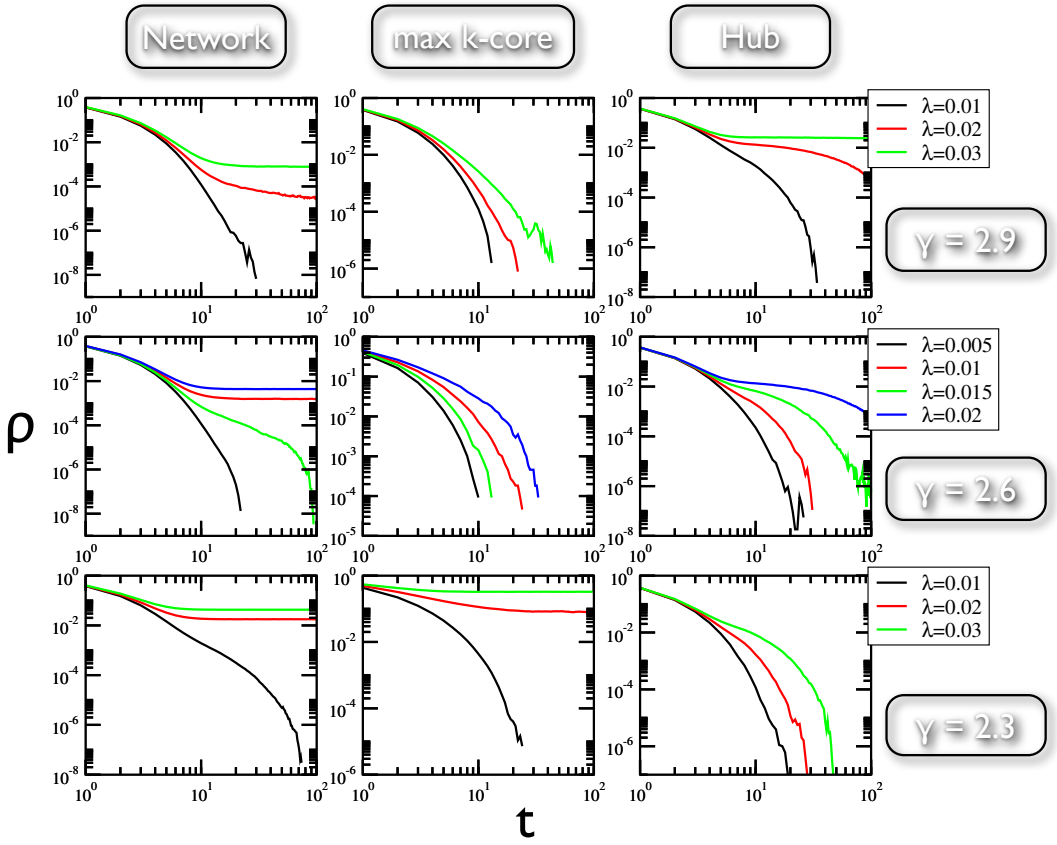

Figure S1: Average density of infected vertices as a function of time, $\rho(t)$, in the SIS model on uncorrelated scale-free networks generated by means of the UCM algorithm. We consider networks with $\gamma = 2.9$, $\gamma = 2.6$ ($N = 3 \times 10^7$) and $\gamma = 2.3$ ($N = 10^6$). The different columns correspond to the average density computed when the dynamics runs over the whole network (left), only over the maximum k-core of the network (center), and only over the largest hub (right), considered as an isolated star network. The different colors correspond to different values of the spreading rate λ. For $\gamma = 2.3$ (bottom row), the onset of the global steady state is correlated with the active state of the epidemics on the maximum k-core, while it corresponds to a subcritical state for the hub. This observation indicates that in this case the maximum k-core is responsible for the overall activity in the network. For large $\gamma > 5/2$, on the other hand, the global active state is linked to an active hub and a subcritical maximum k-core, signaling that it is the former mechanism the one keeping activity on a global scale.

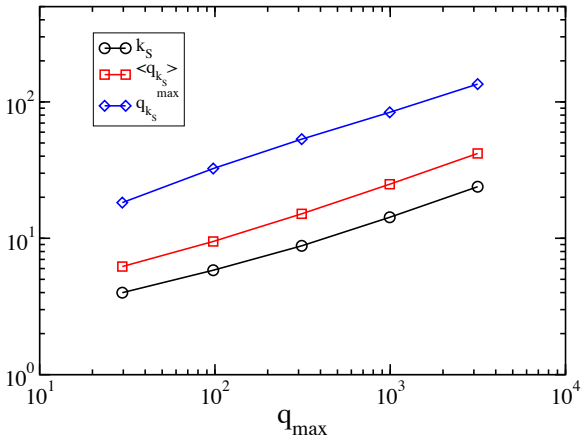

Figure S2: Topological properties of the of the maximum k-core as a function of network size in uncorrelated scale-free networks with degree exponent $\gamma = 2.5$.

4 Degree distributions and correlations in real networks.

In Fig. S3 we report the degree distributions of the three real networks considered. In all cases the distributions decay slowly for large q with an exponent close to $\gamma = 2$.

In Fig. S4(a) we plot on the other hand the average degree of the nearest neighbors (ANN) of a node of degree q for the three real networks considered [4]. The Movies and PGP networks exhibit a mild assortative structure [5]: vertices with high degree tend to be connected in average with vertices of high degree, while low degree vertices are connected to each other. On the contrary, the AS network is strongly disassortative, i.e. vertices with large q are typically connected to nodes with small q, and viceversa. The different strength of degree correlations is highlighted by computing the $\bar{q}_{nn}(q)$ function for the same networks after a randomizing (degree-preserving) procedure is applied [6]: two edges are randomly selected and two vertices at their respective ends are swapped.

While the rewiring procedure completely destroys the weak assortative correlations of the Movies and PGP networks, Fig. S4(b), no effect can be spotted for the AS, indicating

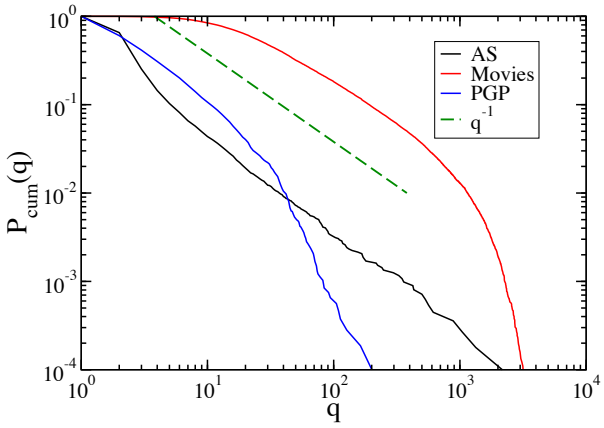

Figure S3: Cumulated degree distribution of the real network datasets considered. All plots show a power-law regime compatible with the form q^{-1}, indicating a degree distribution with a degree exponent $\gamma \sim 2$.

the presence of very strong and robust correlations.

5 Values of the thresholds

The numerical values of the analytical estimates of the different thresholds discussed for the SIS in networks are reported in Table S1. We focus in particular on the networks considered in our manuscript, namely uncorrelated networks generated with the UCM algorithm and three real network datasets. The first column shows the values of $\lambda_c^E = 1/\Lambda_N$, the inverse of the largest eigenvalue of the adjacency matrix. In the second column, we find the value of $1/\sqrt{q_{max}}$, which is the prediction for uncorrelated networks with $\gamma > 5/2$. Finally, the third column presents the value of $\langle q \rangle / \langle q^2 \rangle$, which holds for $\gamma < 5/2$ and coincides with the HMF prediction. We observe that for UCM networks the predictions of Eq. (1) in the manuscript are very well obeyed, indicating that the estimates of Ref. [7] are correct. With regards to real networks, the Movies network shows a threshold in good agreement with the prediction of Eq. (1) for $\gamma < 5.2$, i.e. close to the HMF prediction,

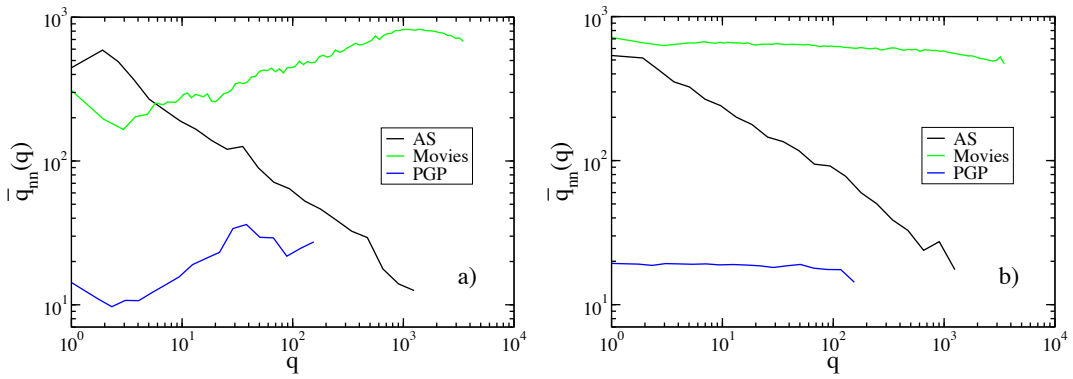

Figure S4: Average degree of the nearest neighbors (ANN) function, $\bar{q}_{nn}(q)$, for the three real networks considered. a) Original networks. b) Randomized networks, under application of the algorithm in Ref. [6].

indicating the relevant role of the maximum k-core. For the PGP network, the agreement with Eq. (1) is not precise, yet the threshold is closer to the HMF prediction and therefore the maximum k-core drives the transition, as shown in Fig. 3 in the manuscript. The opposite is true for the AS network: the inverse of the largest eigenvalue is close to $1/\sqrt{q_{max}}$ and is much larger than the HMF prediction, despite a very slow decay of the degree distribution. The conclusion is that in this case the estimate of Ref. [7] is largely incorrect, thus invalidating Eq. (1). This failure is originated by the disassortative correlations present in AS networks, induced by the presence of a very large hub, which mixes the role of the maximum k-core and the hub in the activation of the epidemics.

To further check the role of correlations and a large hub, we have considered an additional AS map, corresponding to later snapshot of the Internet, and thus characterized by a larger size. The characteristics of this second Internet map (AS2) are the following: $N = 24463$, $\langle q \rangle = 4.2799$, $k_S = 24$, $1/\Lambda_N = 0.01412$ $1/\sqrt{q_{max}} = 0.02012$ $\langle q \rangle / \langle q^2 \rangle = 0.003796$. In Figure S5 we present the results of numerical simulations of the SIS model performed on this AS2 map. We observe that, in this case, for values of λ corresponding to an active global network, neither the hub nor the maximum k-core are apparently in

	$1/\Lambda_N$	$1/\sqrt{q_{max}}$	$\langle q\rangle/\langle q^2\rangle$
	UCM model		
$\gamma = 2.9$, $N = 3 \cdot 10^7$	0.01352	0.01356	0.03896
$\gamma = 2.75$, $N = 3 \cdot 10^7$	0.01308	0.01353	0.02312
$\gamma = 2.6$, $N = 3 \cdot 10^7$	0.01031	0.01351	0.01294
$\gamma = 2.3$, $N = 10^6$	0.01160	0.03168	0.01209
$\gamma = 2.1$, $N = 10^6$	0.00735	0.03163	0.00745
	Real networks		
Movies	0.001223	0.01624	0.00168
PGP	0.02356	0.06984	0.05296
AS	0.016576	0.02045	0.003765

Table S1: Table of SIS thresholds for synthetic and real networks.

the active phase. This result, which is also found in other AS maps we have considered, confirms that the presence of very strong correlations alters the clear picture observed in uncorrelated networks, leading to a mixing of the activation mechanisms.

6 SIS dynamics on Weber-Porto networks.

Recently, Weber and Porto [8] have introduced a modified configuration model [9] which allows to generate graphs with a given degree distribution and, simultaneously, a predetermined ANN function $\bar{q}_{nn}(q)$. We have performed simulations of the SIS dynamics on networks generated by the Weber-Porto method, and compared the density of active nodes as a function of λ when the dynamics takes place on the whole network or only on the maximum k-core or on a star-graph with $q_{max}+1$ nodes, where q_{max} is the degree of the largest hub. Numerical values of the different theoretical thresholds, for different values of the degree exponent γ and of the exponent α of the ANN function, $\bar{q}_{nn}(q) \sim q^{\alpha}$,

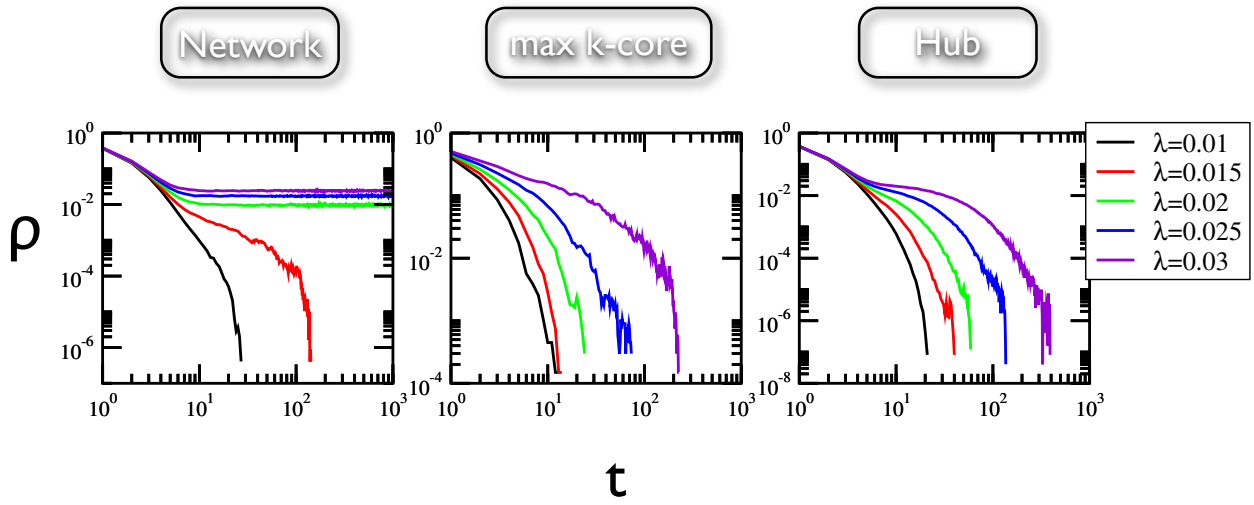

Figure S5: Average density of infected vertices as a function of time, $\rho(t)$, in the SIS model on the AS2 Internet map. The different columns correspond to the average density computed when the dynamics runs over the whole network (left), only over the maximum k-core of the network (center), and only over the largest hub (right), considered as an isolated star network. The different colors correspond to different values of the spreading rate λ.

are reported in Table S2. Positive values of α imply assortative correlations, while $\alpha < 0$ is the signature of disassortative correlations. Results of numerical simulations are presented in Fig. S6.

	$1/\Lambda_N$	$1/\sqrt{q_{max}}$	$\langle q \rangle / \langle q^2 \rangle$
	Weber-Porto network model		
$\gamma = 2.1$, $\alpha = 0.5$	0.008548	0.05634	0.01798
$\gamma = 3.5$, $\alpha = -0.5$	0.064435	0.06482	0.14492
$\gamma = 2.1$, $\alpha = -0.5$	0.016137	0.01754	0.00353
$\gamma = 3.5$, $\alpha = 2$	0.021856	0.07001	0.14675

Table S2: Table of SIS thresholds for Weber-Porto networks.

In the first two cases presented in Table S2, correlations are expected to strengthen the mechanism already driving the transition for uncorrelated networks: indeed for $\gamma > 5/2$ disassortative correlations make the network more "star-like", while for $\gamma < 5/2$ assortative correlations are expected to make the max k-core play an even more important role. This is confirmed by the data in Table S2:

- For $\gamma = 2.1$ and $\alpha = 0.5$, the threshold $1/\Lambda_N$ is smaller than the HMF prediction (which is in its turn smaller than $1/\sqrt{q_{max}}$).
- For $\gamma = 3.5$ and $\alpha = -0.5$ the threshold $1/\Lambda_N$ is in very good agreement with $1/\sqrt{q_{max}}$.

Eq. (1) in the manuscript turns out to be essentially correct. Numerical results in Supplementary Figure S6 confirm these findings. Notice that for $\gamma = 3.5$ and $\alpha = -0.5$ there is no k-core structure in the network. Numerical results (Fig. S6) confirm these findings.

In the other two cases, correlations act against the mechanism at work on uncorrelated networks. Are they able to completely perturb the picture and change the activation mechanism of the epidemics?

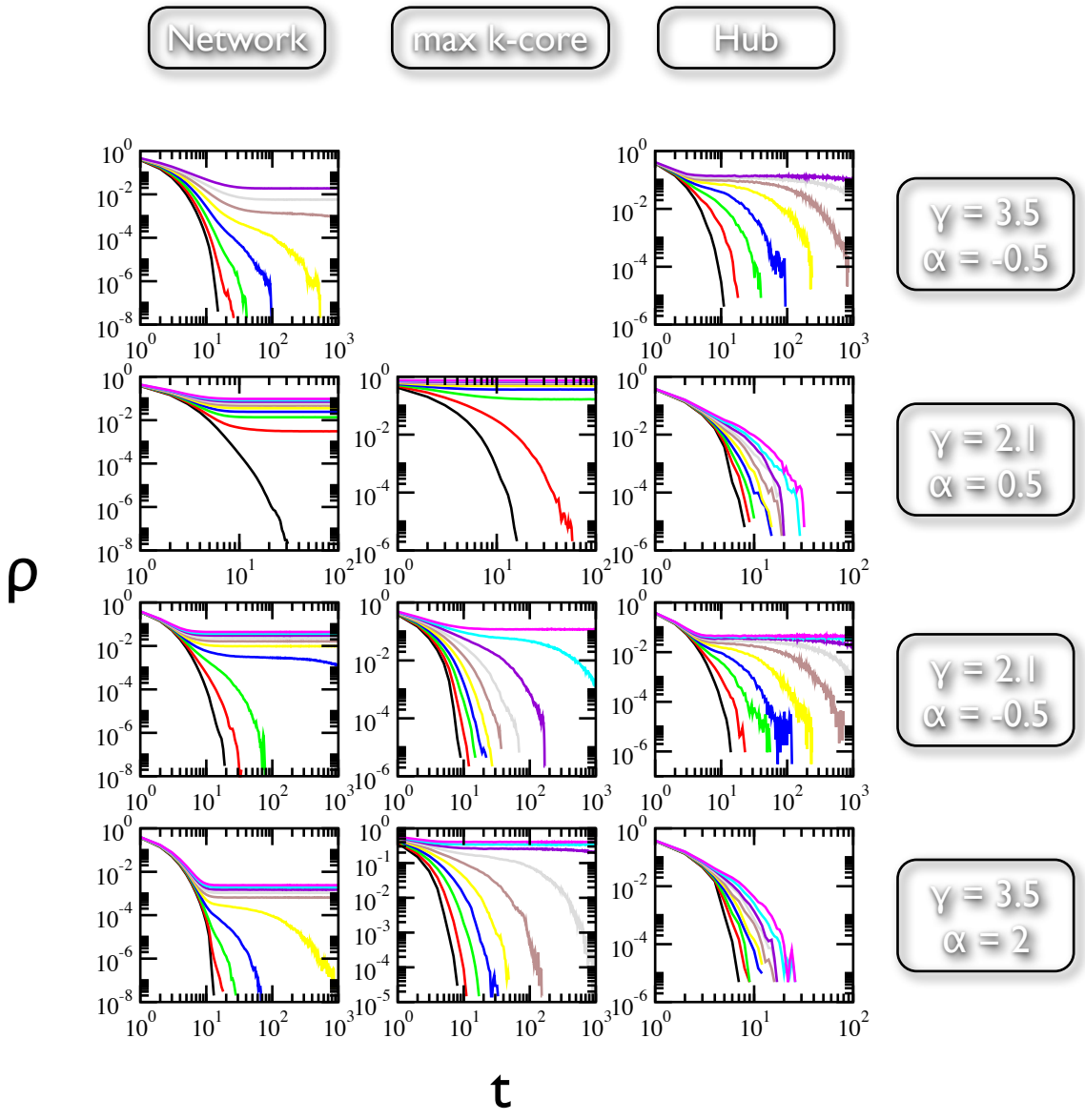

Figure S6: Density of infected vertices as a function of time in the SIS model on Weber-Porto networks with different values of γ and α. Network sizes $N = 10^4$. We plot the average density over the whole network (left column), over the maximum k-core (center column), and over the largest hub (right columns). The different colors correspond, from bottom to top of each plot, to increasing values of the spreading rate λ.

- For $\gamma = 2.1$ and disassortative networks ($\alpha = -0.5$), the threshold $1/\Lambda_N$ is larger than the HMF prediction and it coincides with $1/\sqrt{q_{max}}$. This indicates that the largest hub drives the global transition, at odds with the prediction of Eq. (1). Here correlations change completely the behavior, leading to a violation of the estimate of Λ_N on Ref. [7]. The direct numerical simulations, presented in Figure S6, confirm these findings.

- For $\gamma = 3.5$ and assortative correlations ($\alpha = 2$), the threshold $1/\Lambda_N$ is much smaller than $1/\sqrt{q_{max}}$ (which is in its turn smaller than the HMF prediction). This shows again that the result of Ref. [7] does not hold. The direct numerical simulations, Figure S6, clearly shows that it is the maximum k-core which triggers the transition in this case.

References

[1] Pastor-Satorras, R. & Vespignani, A. Epidemic spreading in scale-free networks. *Phys. Rev. Lett.* **86**, 3200–3203 (2001).

[2] Catanzaro, M., Boguñá, M. & Pastor-Satorras, R. Generation of uncorrelated random scale-free networks. *Phys. Rev. E* **71**, 027103 (2005).

[3] Castellano, C. & Pastor-Satorras, R. Thresholds for epidemic spreading in networks. *Phys. Rev. Lett.* **105**, 218701 (2010).

[4] Pastor-Satorras, R., Vázquez, A. & Vespignani, A. Dynamical and correlation properties of the Internet. *Phys. Rev. Lett.* **87**, 258701 (2001).

[5] Newman, M. E. J. Assortative mixing in networks. *Phys. Rev. Lett.* **89**, 208701 (2002).

[6] Maslov, S. & Sneppen, K. Specificity and stability in topology of protein networks. *Science* **296**, 910–913 (2002).

[7] Chung, F., Lu, L. & Vu, V. Spectra of random graphs with given expected degrees. *Proc. Natl. Acad. Sci. USA* **100**, 6313–6318 (2003).

[8] Weber, S. & Porto, M. Generation of arbitrarily two-point-correlated random networks. *Phys. Rev. E* **76**, 046111 (2007).

[9] Molloy, M. & Reed, B. A critical point for random graphs with a given degree sequence. *Random Struct. Algorithms* **6**, 161 (1995).